Effect of Geometric Parameters on Exterior Wall-Floor Connection

S .Greeshma. & K.P. Jaya
Anna Universiy, Chennai

SUMMARY
The floor slabs and shear walls together act as a rigid jointed frame in resisting gravity loads and lateral forces due to wind and earthquake. The junction between the wall and slab is a key force resisting element which is subjected to severe stress concentration. This paper presents the results of a parametric study of shear wall – floor slab connection under lateral cyclic loading. To carry out the analytical investigations, the structure was modelled in a Finite Element software ANSYS. The specimens were sorted into two groups based on the ratio of height of shear wall and the effective width of the slab (H/W_e). Four exterior shear wall - slab joint sub assemblages were analyzed for different thickness ratio of slab and shear wall (t_s/t_w). The optimum parameters such as height of shear wall (H), effective width of the slab (W_e), thickness of shear wall (t_w) and slab (t_s) were found out from the analysis. The analytical results of the optimum parametric model are validated by conducting experiments. Good correlation was found between analytical and experimental results.

Keywords: shear wall, floor slab, cyclic load, parametric model.

1. INTRODUCTION

Traditionally reinforced concrete shear walls have been used as lateral-load resisting systems in multistory buildings. The floor slabs and shear walls together act as a rigid jointed frame in resisting gravity loads and lateral loads due to wind and earthquake. Lateral loads cause vertical shears along the line of contraflexure in the floor slabs which is finally transmitted to the walls through the floor slab. The junction between the wall and the slab is subjected to severe stress concentration. This problem has already been studied theoretically by Coull and Wong (1985) to determine the distribution of shear stresses at the junction. Memon (1984) produced charts for determination of design moments in coupling slabs due to lateral loads. Bhatt et al.(1986) tested the RCC models with vertical bars around the wall periphery as shear reinforcement. Vinoth et al.(2009) presented results of experimental behaviour of wall-slab joint in a laterally loaded shear wall building. The object of the present investigation is to investigate the effect of various geometric parameters like height of shear wall (H), effective width of the slab (W_e), thickness of slab (t_s) and thickness of shear wall (t_w) on the behaviour of exterior shear wall – floor slab connection subjected to reversible cyclic loading.

2. ANALYTICAL MODEL

A six storied R.C. building with exterior shear wall (12 m x 7.5 m in plan) is modeled, analyzed and designed using ETABS software. Having designed the structure, the shear wall – slab joint is subjected to finite element analysis and experimental investigation. Since the analytical model has to be validated through experimental results, a scale factor of four has been adopted for both analytical and experimental model. Thus the original structure has been reduced four times following the laws of similitude. Following the laws of similitude, the reinforcements are also reduced to $1/4^{th}$ of the design areas of the reinforcements of the prototype as shown in Table 2.1.

Table 2.1. Reinforcement details of Shear wall, Slab and Joint

Shear wall	Vertical bars	24 nos - Φ 6 (2 layers)
	Horizontal bars	Φ6 @ 60 mm c/c for a distance of 167 mm at either side of joint and 120 mm c/c for remaining portion
	Stirrups	Φ3 @ 60 mm c/c through out the entire length of the shear wall for a distance of 167 mm from either side of joint and Φ3 @ 120 mm c/c is restricted within the boundary length of the shear wall for remaining portion.
Slab	Longitudinal bars –Along the direction of shear wall.	Φ6 @ 62 mm c/c for a distance of 70 mm from the slab end and 90 mm c/c for the remaining length.
	Transverse bars – Perpendicular to the direction of shear wall.	Φ6 @ 54 mm c/c for a distance of 61.5 mm from the slab end and 100 mm c/c for the remaining length.
Joint	Transverse Reinforcement	Φ3 @ 30 mm c/c.
		Confining reinforcement at joint is as per provisions given for Beam –Column joint in IS 13920:1993 along with the provision of additional U hooks for the effective width (W_e) of the slab.

3. PARAMETERS STUDIED

The parameters considered for the present study are the ratio of height of shear wall to effective width of the slab (H/W_e) and thickness ratio of slab to shear wall (t_s/t_w).

3.1 Height of Shear Wall to Effective Width ratio (H/W_e)

The specimens are sorted into two types based on the ratio of height of shear wall and the effective width of the slab (H/W_e) such as 2.25 and 2.8. Height of shear wall is considered to be same for all the specimens and is 875 mm for $1/4^{th}$ scale model. The effective width of the slab is the width of the slab adjacent to the shear wall that is used to resist the collector forces. The procedures outlined in "Seismology and Standards Committee (2005)" propose two methods to determine the effective slab width.

3.2 Ratio of Thickness of Slab to Shear Wall (t_s/t_w)

Thickness of shear wall is considered to be same for all the specimens and is 75 mm where as thickness of slab considered are 50 mm and 62.5mm, leading to t_s/t_w ratios as 0.667 and 0.833 respectively.

4. DESCRIPTION OF PARAMETRIC MODEL

The models are designated as Type 1 (H/W_e = 2.8) and Type 2 (H/W_e = 2.25) and are detailed as shown in Figure 4.1 and Figure 4.2.

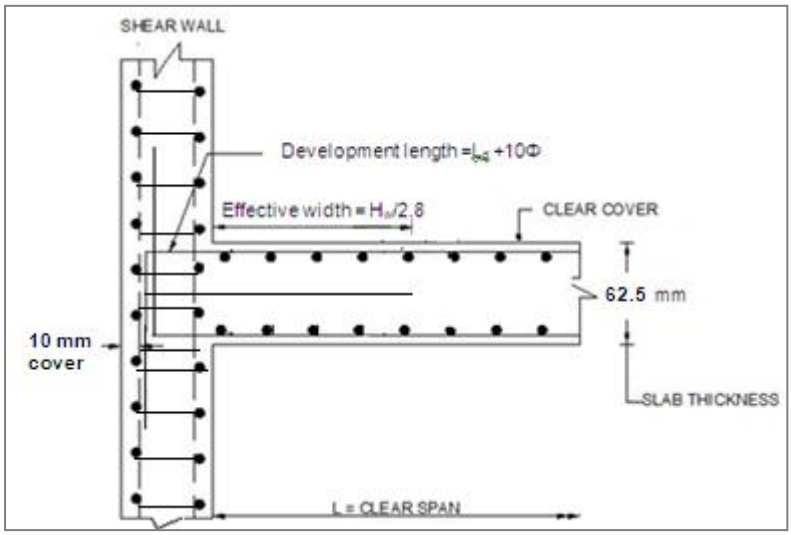

Figure 4.1. Shear wall – slab joint for Type 1 Model

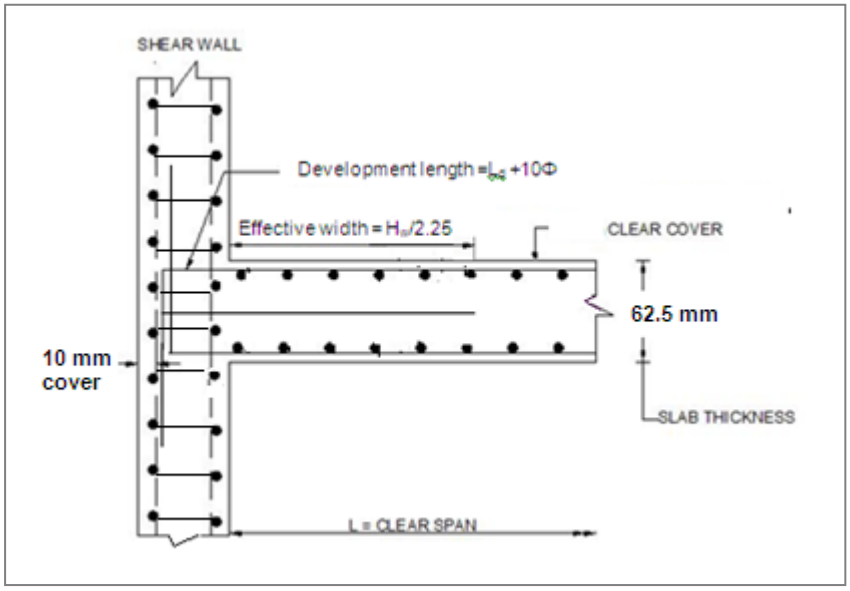

Figure 4.2. Shear wall – slab joint for Type 2 Model

5. MODELLING OF SHEAR WALL – FLOOR SLAB CONNECTION

For analytical modeling of shear wall – slab connection, ANSYS Multiphysics (Version11) was used. The elements used were SOLID 65 for concrete and LINK 8 for reinforcement modeling. The material properties for modeling the wall – slab joint have been adopted according to Wolanski (2004). The average 28-day cube strength (f_{cu}) of concrete is 44.22 MPa. The relationship of cylinder strength (f_c') and cube strength (f_{cu}) given by the ACI Code as (f_c' =0.8 f_{cu}) and thus the ultimate compressive strength (f_c') was 35.376 MPa. The uniaxial stress-strain relationship for concrete developed by Desayi and Krishnan (1964), which is given by Eqn.(5.1), was adopted for modeling concrete.

$$f = \frac{E\varepsilon}{1+\left(\frac{\varepsilon}{\varepsilon_0}\right)^2} \tag{5.1}$$

Where, f = stress at any strain ε and ε_0 = strain at the ultimate compressive strength f_c'

E = a constant (same as initial tangent modulus) such that $E = \frac{2f_c'}{\varepsilon_0}$

5.1 Boundary Conditions

The shear wall is assumed to be fixed at the base. For this all dofs are constrained at the base of the shear wall. At the slab end, all the degrees of freedom are constrained except in-plane displacement and rotations θ_x and θ_z as shown in Figure 5.1. The shear wall – slab joint is subjected to varying lateral load (reversible cyclic load) at the end of the slab as shown in Figure 5.2.

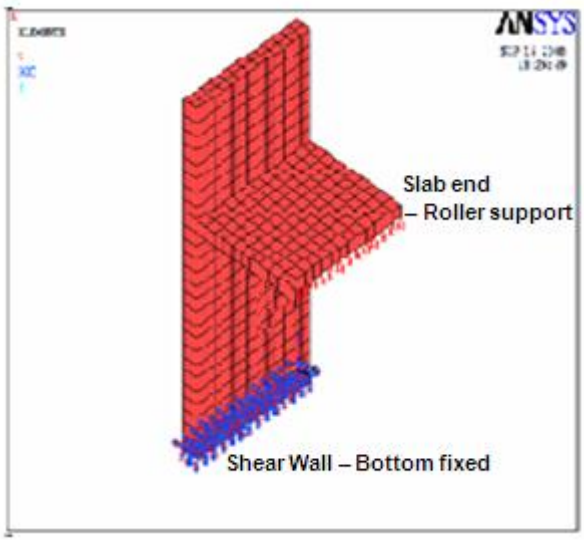

Figure 5.1. Displacement boundary conditions

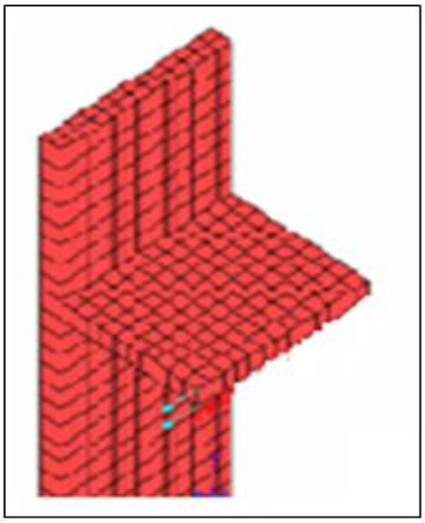

Figure 5.2. Force boundary conditions

The loading is controlled by drift ratio for both the models as illustrated in Figure 5.3 (Hwang et al.(2005), where the drift ratio is defined as the deflection of the load point divided by the distance between the load point and the centre line of the shear wall.

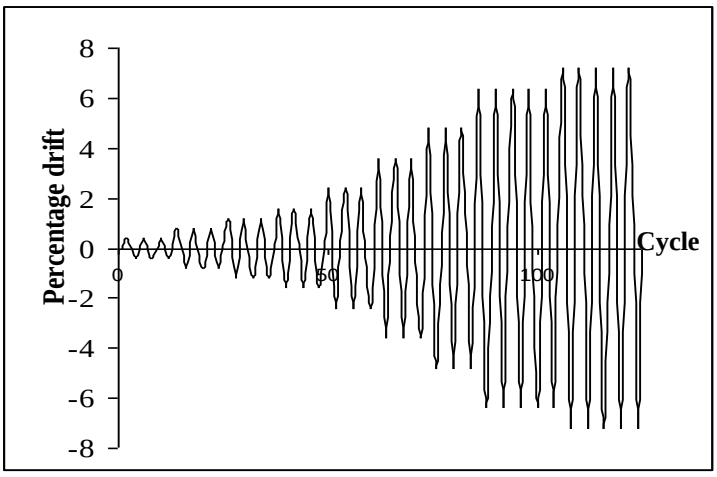

Figure 5.3. Loading history

6. FINITE ELEMENT ANALYSIS

The finite element analysis has been carried out for the shear wall- slab joint subjected to cyclic lateral drift histories. The displacement convergence criterion was used with the tolerance of 0.001. The command prompt line input data was adopted for applying the reversible cyclic loading. The analysis type has been mentioned as transient.

7. EXPERIMENTAL INVESTIGATION

The experimental investigations were carried out at Structural Dynamics Laboratory, Structural Engineering Division, Anna University, Chennai. The specimens are tested in a well equipped set up and given static reverse cyclic loading. To apply the simulated cyclic load on the specimen, 100 kN capacity hand-controlled screw jacks (Two Nos) was connected to a reaction steel frame. The bottom of the shear wall surface was attached to two steel channels using 4 high strength threaded rods (in two layers). The two base channels were, in turn, fastened to two strong I-beam. The latter was post-tensioned to the lab floor using four high strength post-tensioning rods. Specimens were tested for static reverse cyclic loading applied at the end of the slab. A constant axial load of 5 T was applied at an eccentricity of 0.5 m by means of hydraulic jack (40 T capacity) mounted vertically to the loading frame (100 T) to simulate the axial load and moment at the mid height of the shear wall from the joint assembly. The slab end was given an external hinge support, which was fastened to the strong reaction floor. A schematic view of the test setup is shown in Figure 7.1. The experimental set-up at laboratory is shown in Figure 7.2.

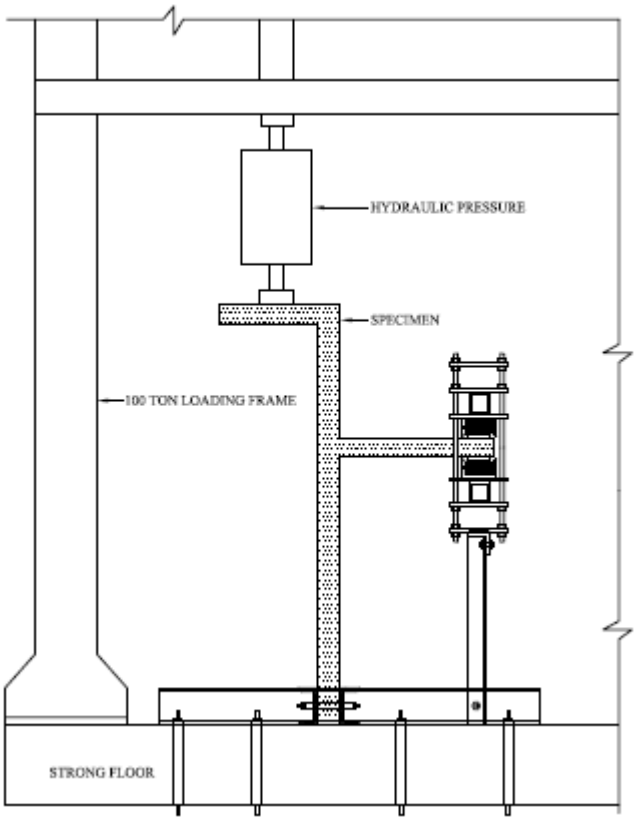

Figure 7.1. Schematic View of Test Set-up (Rear View)

Figure 7.2. Experimental Set-up at Laboratory

8. ANALYTICAL RESULTS AND DISCUSSIONS

Finite element analysis is carried out for both the types of models with t_s/t_w =0.833. The results of the analysis are presented as follows.

8.1 U1timate Load Carrying Capacity

The variation in ultimate load carrying capacity for the models for positive and negative direction of loading is shown in Table 8.1. It is observed that the ultimate load is higher for Type 2 model.

Table 8.1. Ultimate load carrying capacity of specimens

Designation of specimen	Ultimate Load (kN)		
	Positive direction	Negative direction	Average (P_u)
Type 1	24.520	23.152	23.836
Type 2	26.862	26.675	26.768

The increase in ultimate load for Type 2 model can be attributed due to the presence of reinforcement in the critical sections (for higher effective width of H/2.25) which experience higher shear and flexural stresses due to cyclic loading.

8.2 Load – Drift Hysteretic loops

The hysteretic behaviour of Type 1 model shows a moderate level of pinching, which may be attributed to inadequate confinement in the connection region. In addition, the Type 1 specimen showed a sudden decrease in strength. However Type 2 specimens exhibited large, stable loops throughout the test with little strength or stiffness degradation (Figure 8.1).

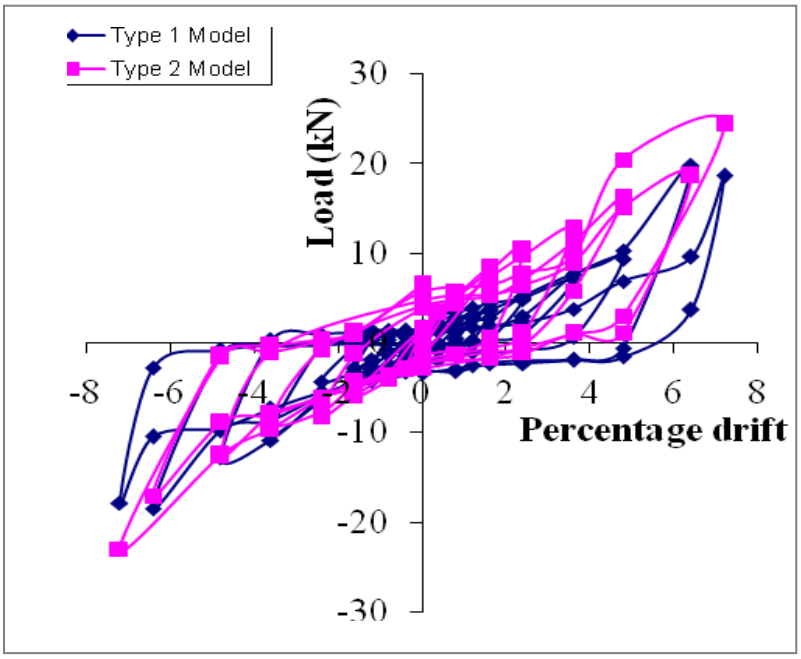

Figure 8.1. Load versus drift curve of specimens

(iii) Energy dissipation

Cumulative energy absorbed during each cycle of loading is plotted against corresponding cycle for Type 1 and Type 2 models as shown in Figure 8.2. It is observed that Type 2 model exhibits higher energy dissipation capacity compared to Type 1 model. The reinforcement (U bars) passing through the joint had less robust anchorage for Type 1 model. In the case of Type 2 model, the anchorage of U bars passing through the connection was excellent.

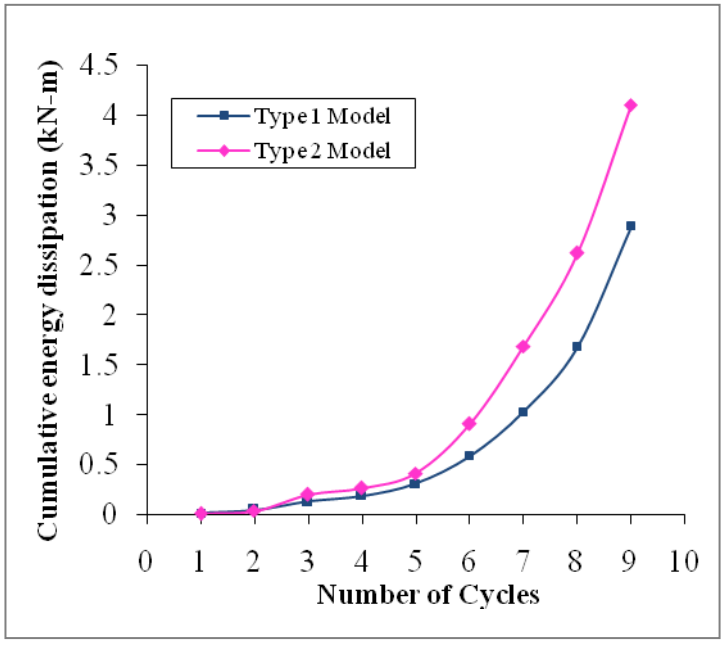

Figure 8.2. Cumulative energy dissipation curves of specimens

From the above results, it is observed that Type 2 model had exhibited higher ultimate strength and energy dissipation capacity when compared to Type 1 model. Hence a further parametric study with respect to thickness ratio has been carried out for Type 2 model alone.

The variation in ultimate load for Type 2 model with the ratio of slab/wall thickness is shown in Table 8.2. It is observed that the models with t_s/t_w of 0.833 performed better when compared to model with t_s/t_w of 0.667.

Table 8.2. Ultimate load carrying capacity of Type 2 model

Slab/Wall Thickness	Ultimate Load (kN)		
	Positive direction	Negative direction	Average (P_u)
t_s/t_w =0.667	23.820	24.315	24.067
t_s/t_w =0.833	26.862	26.675	26.768

The cumulative energy dissipation capacity of Type 2 model for various t_s/t_w ratio is shown in Figure 8.3. The increase in the ratio t_s/t_w increases the energy dissipation of the connection. It is because; the increase in ratio t_s/t_w result in a significant reduction in the large bending moment factors in the slab adjacent to the wall.

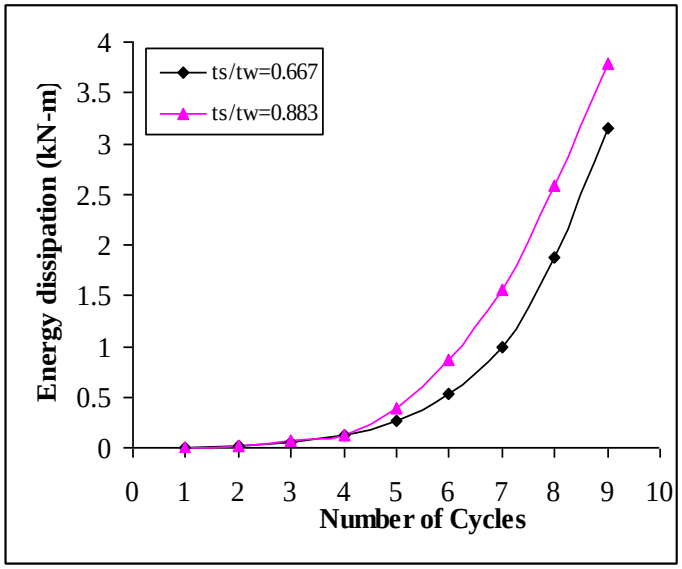

Figure 8.3. Cumulative energy dissipation curves of Type 2 model with different t_s/t_w ratio

9. EXPERIMENTAL VALIDATION

From the above parametric study, it is observed that Type 2 model with t_s/t_w of 0.833 had exhibited higher ultimate strength and energy dissipation capacity when compared to that with t_s/t_w of 0.667 as well as Type 1 model. Hence further experimental validation has been carried out for Type 2 model with t_s/t_w of 0.833 alone.

9.1 Ultimate Load Carrying Capacity

The variation in ultimate load carrying capacity for Type 2 model with t_s/t_w of 0.833 from analytical and experimental study is shown in Table 9.1. It is observed that the experimental ultimate load is matching well with the analytical load and the variation is marginal (<1%).

Table 9.1. Ultimate load carrying capacity of specimens

Specimen Designation	Thickness Ratio	Ultimate Load (kN) (Analytical)	Ultimate Load (kN) (Experimental)
Type 2	t_s/t_w =0.833	26.862	26. 971

9.2 Load – Drift Hysteretic loops and Energy Dissipation

A relative comparison of load – drift hysteretic loop for Type 2 model is shown in Figure 9.1. The load – drift curve follows almost the same path as that of analytical one. The trend in variation is also same. The cumulative energy dissipation curves are presented in Figure 9.2.

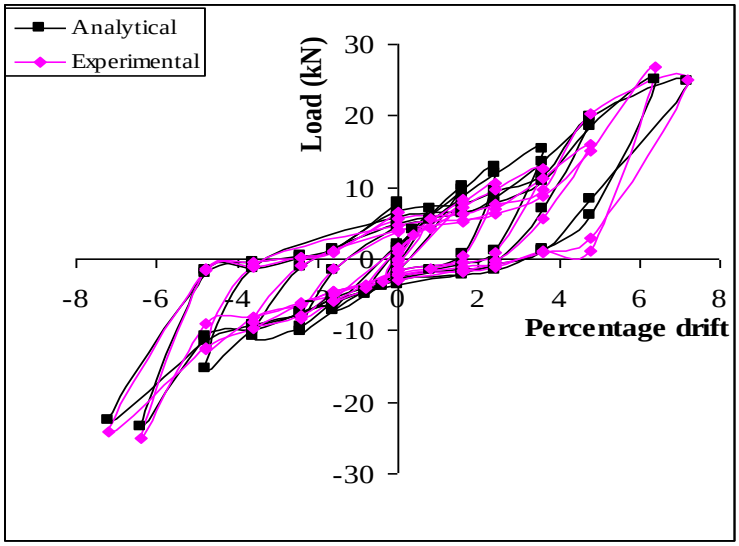

Figure 9.1. Load versus drift curve of Type 2 model

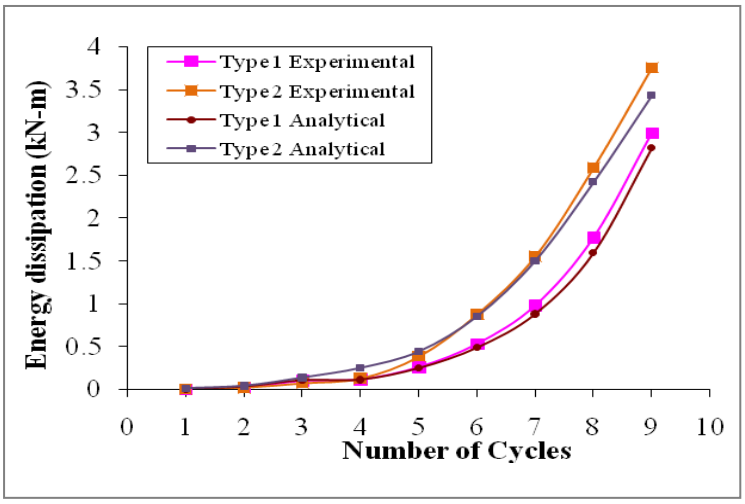

Figure 9.2. Cumulative energy dissipation curves of specimens

All the above results show that the experimental results agree well with the analytical results. Further they also show that the best performance of the joint is obtained for Type 2 model with t_s/t_w =0.833.

10. CONCLUSIONS

The results of the study, presented in this paper, establish the effect of different parameters like ratio of height of shear wall to the effective width of the slab (H/W_e) and slab to shear wall thickness (t_s/t_w) on the behavior of exterior shear wall – slab joints. The shear wall and the slab has been modelled using ANSYS software, using Solid65 element and Link8 element. Following are the conclusions drawn based on the analytical modelling and experimental investigations carried out to study the effect of parameters on the behaviour of shear wall-slab joint under cyclic loading.

1) With respect to load carrying capacity from the analytical study, the model has exhibited higher ultimate strength when the confining U hooks are extended for an effective width of H/2.25 (Type 2) when compared with H/2.8 (Type 1). It is observed that the ultimate strength for Type 2 model is 12.3 % higher than that of Type 1 model.
2) Spindle-shaped hysteretic loops are observed with large energy dissipation capacity for Type 2 model compared to Type 1 model. The enhancement in energy dissipation for Type 2 model is observed to be 21.68 % higher than that of Type 1 model.
3) From all these observations, it is concluded that Type 2 model exhibited very good performance with respect to ultimate load capacity and energy dissipation capacity when compared to Type 1. Hence further parametric studies are carried out on Type 2 model by varying slab to wall thickness ratio (t_s/t_w).
4) It is observed that the ultimate strength increased for t_s/t_w=0.883 when compared to t_s/t_w=0.667. The increase in ultimate strength for Type 2 model is 11.3 % higher than that of Type 1 model. The deformation capacity is also observed to be higher for model with t_s/t_w=0.883 when compared to t_s/t_w = 0.667. The deformation capacity for model with t_s/t_w=0.883 is 18.75 % higher than that with t_s/t_w = 0.667.
5) The analytical results with respect to ultimate load are matching well with the experimental load. The maximum variation in energy dissipation is observed to be for Type 2 model and is within 10%.

ACKNOWLEDGEMENT

The authors thank the Technical staff of the Laboratories in Structural Engineering Division, Anna University Chennai for the assistance provided in conducting the experimental studies. The research sponsorship from UGC (University Grants Commission, Government of India) under Major Research Scheme is greatly acknowledged.

REFERENCES

ACI Committee 318. (2002). Building Code Requirements for Structural Concrete (ACI 318-02). American Concrete Institute. Detroit.

ANSYS.(2011).ANSYS User's Manual Revision 11. ANSYS, Inc.

Bhatt, P., Memon, M. and Bari, S. (1986). Strength of plane shear wall – floor slab junction. Proceedings of *International symposium on fundamental theory of reinforced and prestressed concrete*, Nanjing, China, **Vol III:**541-549.

Coull,A. and Wong, Y.C. (1985). Effect of local elastic wall deformations on the interaction between floor slabs and flanged shear walls. *Journal of Building and Environment*, **20:3**, 169-179.

Desai, P. and Krishnan, S. (1964). Equation for the stress-strain curve of concrete, *ACI Structural Journal*, **61:22**, .345-350.

ETABS (Version 9). ETABS User's Manual.

Memon,M. (1984). Determination of Design Moments in Connecting Slabs. *Mehran University Research Journal of Engineering and Technology*,.**4:1**, 6-10.

Memon,M. and Narwani,T.D.(2008). Experimental Investigations Regarding Behaviour of Tall Buildings Subjected to Lateral Loading. *Journal of Quality and Technology Management*, **4:1**, 39-50.

SEAONC Seismology and Structural Standards Committee.(2005). Seismology Publication.

Hwang,S.J., Hung-Jen L., Ti-Fa L., Kuo-Chou W. and Hsin-Hung T. (2005). Role of hoops on shear strength of reinforced concrete beam-column joints. *ACI Structural Journal*, **102:3**, 445-453.

Wolanski,A.J. (2004). Flexural behavior of reinforced and prestressed concrete beams using finite element Analysis, A Thesis submitted to the Faculty of the Graduate School, Marquette University, Milwaukee, Wisconsin, 1-67.